JOURNAL OF VIROLOGY, Apr. 2009, p. 3568–3580 Vol. 83, No. 8
0022-538X/09/$08.00+0 doi:10.1128/JVI.02238-08

Amino Acid Residues in the Fusion Peptide Pocket Regulate the pH of Activation of the H5N1 Influenza Virus Hemagglutinin Protein▽

Mark L. Reed,[1] Hui-Ling Yen,[1]† Rebecca M. DuBois,[1] Olga A. Bridges,[1] Rachelle Salomon,[1]‡ Robert G. Webster,[1] and Charles J. Russell[1,2]*

Division of Virology, Department of Infectious Diseases, St. Jude Children's Research Hospital, 262 Danny Thomas Place, Memphis, Tennessee 38105-3678,[1] and Department of Molecular Sciences, University of Tennessee, Memphis, Tennessee 38163[2]

Received 23 October 2008/Accepted 19 January 2009

The receptor specificity and cleavability of the hemagglutinin (HA) protein have been shown to regulate influenza A virus transmissibility and pathogenicity, but little is known about how its pH of activation contributes to these important biological properties. To identify amino acid residues that regulate the acid stability of the HA protein of H5N1 influenza viruses, we performed a mutational analysis of the HA protein of the moderately pathogenic A/chicken/Vietnam/C58/04 (H5N1) virus. Nineteen HA proteins containing point mutations in the HA2 coiled-coil domain or in an HA1 histidine or basic patch were generated. Wild-type and mutant HA plasmids were transiently transfected in cell culture and analyzed for total protein expression, surface expression, cleavage efficiency, pH of fusion, and pH of conformational change. Four mutations to residues in the fusion peptide pocket, Y23H and H24Q in the HA1 subunit and E105K and N114K in the HA2 subunit, and a K58I mutation in the HA2 coiled-coil domain significantly altered the pH of activation of the H5 HA protein. In some cases, the magnitude and direction of changes of individual mutations in the H5 HA protein differed considerably from similar mutations in other influenza A virus HA subtypes. Introduction of Y23H, H24Q, K58I, and N114K mutations into recombinant viruses resulted in virus-expressed HA proteins with similar shifts in the pH of fusion. Overall, the data show that residues comprising the fusion peptide pocket are important in triggering pH-dependent activation of the H5 HA protein.

Highly pathogenic influenza H5N1 viruses, first observed in humans in Hong Kong in 1997 and 1998 (8), have since been reported in repeated outbreaks in Asia, Africa, and Europe, resulting in the culling of millions of infected poultry and an estimated worldwide economic cost of more than $10 billion (reviewed in references 23 and 34). As of December 2008, the transmission of H5N1 influenza viruses from birds to humans has resulted in 246 fatalities from 389 reported cases (www.who.int/csr/disease/avian_influenza/en/). An understanding of the molecular properties of emerging H5N1 influenza viruses may assist in future surveillance and containment strategies.

The influenza A virus hemagglutinin (HA) protein helps determine transmissibility and pathogenicity by its receptor binding and membrane fusion functions during viral entry. The HA protein is synthesized as uncleaved HA0 monomers, with trimerization and correct folding of the protein necessary for its trafficking to the cell surface (14). Cleavage of the HA0 precursor into subunits HA1 and HA2 is a prerequisite for activation of the HA protein to cause membrane fusion (24, 26). In highly pathogenic H5 and H7 subtypes of influenza A viruses, the presence of a polybasic cleavage site allows ubiquitous enzymes in the trans-Golgi network to cleave the HA protein, thereby facilitating systemic infection and causing greater pathogenicity (12, 32, 47). During entry of the influenza virus, the HA protein binds to sialic acid-containing receptors on the surface of the host cell (48). Receptor specificity contributes to virus host range: avian influenza viruses typically bind with a higher affinity to α(2,3) sialosides, whereas human influenza viruses preferentially bind to the α(2,6) sialic acid form (5, 31). After binding to the receptor on the target cell membrane, the virion is internalized by endocytosis (48). Within the endosomal compartment, the virion is exposed to increasingly low pH. At a threshold pH, which varies among strains and is typically between 5 and 6 (7), the HA protein undergoes an irreversible conformation change from its metastable prefusion conformation to a low-pH hairpin structure, promoting fusion of the virion and endosomal membranes (3). A change in the pH of fusion can help influenza viruses adapt to different host species and cell lines (15, 27), as well as facilitate resistance to antiviral agents that raise endosomal pH at high concentrations (7, 9, 39–41). However, a very high pH of fusion may facilitate environmental inactivation of the virus (1), and a very low one may cause lysosome-mediated degradation of the virus (53).

Previous studies using amantadine selection and laboratory adaptation to different host cells identified mutations in the HA proteins of H3 and H7 influenza subtypes that alter the pH at which fusion is triggered (6, 7, 9, 13, 21, 27, 39–41, 46). Residues that regulate the acid stability of H3 and H7 HA proteins are located in four broad regions: (i) the fusion peptide comprising the first 25 N-terminal residues of the HA2

* Corresponding author. Mailing address: Department of Infectious Diseases, MS 330, St. Jude Children's Research Hospital, 262 Danny Thomas Place, Memphis, TN 38105-3678. Phone: (901) 595-5648. Fax: (901) 595-8559. E-mail: charles.russell@stjude.org.

† Present address: Department of Microbiology, The University of Hong Kong, University Pathology Building, Queen Mary Hospital, Pokfulam Road, Hong Kong.

‡ Present address: Division of Microbiology and Infectious Diseases, NIAID/NIH/DHHS, 6610 Rockledge Dr., Bethesda, MD 20817.

▽ Published ahead of print on 4 February 2009.

subunit (6, 7, 21, 40); (ii) the fusion peptide pocket, comprising residues residing within both HA subunits that surround the fusion peptide within the neutral pH metastable conformation (7, 39, 46); (iii) the coiled-coil regions of the HA2 subunit (7, 39); and (iv) the interface between the HA1 and HA2 subunits (7). These residues may also contribute to the acid stability of the HA protein by changing local interactions in structural regions important in regulating intermediate steps in the fusion conformational change (49).

High-resolution structures have been determined for multiple HA subtypes in recent years (11, 16, 35, 42, 43, 51, 52). Alignments of structures of different subtypes have revealed marked structural differences, such as rotation of the HA1 subunit around the central axis of the HA2 subunit and the shape and orientation of smaller structural elements such as the HA2 subunit membrane distal loop (16). HA proteins from all 16 known subtypes can be classified into five structural clades on the basis of these structural differences and signature sequences (35). In this structural phylogeny, the H5 HA protein lies distinct from the H3 and H7 subtypes (42, 52), raising the possibility that the pH-dependent activation of the H5N1 HA protein may be regulated differently than the H3 and H7 HA proteins.

To investigate the role of individual amino acids and potential mechanisms that modulate the acid stability of the H5 HA protein, 19 point mutations were made within the H5 HA protein of A/chicken/Vietnam/C58/04 (C58). The effects of the mutations on HA protein expression, cleavage, and the pH of membrane fusion and HA protein conformational changes are consistent with amino acid residues in the fusion peptide pocket playing a major role in regulating the pH of activation of the H5N1 HA protein.

MATERIALS AND METHODS

Plasmids. Point mutations were introduced into plasmid pSH054-A/chicken/Vietnam/C58/04 HA (36) by using a QuikChange site-directed mutagenesis kit (Stratagene, La Jolla, CA) according to the manufacturer's instructions. Residues are identified by H5 numbering throughout the study. Wild-type and mutant HA genes were subcloned into a pCAGGS expression plasmid (45) using XhoI and ClaI restriction enzyme sites. Nucleotide sequences of all plasmids were verified by DNA sequencing at the Hartwell Center for Bioinformatics and Biotechnology, St. Jude Children's Research Hospital.

Cell culture. Monolayer cultures of Vero cells (ATCC CCL-81), BHK-21 cells (ATCC CCL-10), and BSR-T7/5 cells (2) were grown in Dulbecco modified Eagle medium (DMEM) supplemented with 10% fetal bovine serum, 1% glutamine, 1% penicillin, and 1% streptomycin. BSR-T7/5 cells were also grown in the presence of G418 (final concentration, 1 mg/ml), which was added to the DMEM at every other passage. BHK-21 cells were also supplemented with 10% tryptose phosphate broth.

Viruses. Recombinant viruses containing mutations Y23H, H24Q, K58I, and N114K were generated as described previously (19, 36). Briefly, eight dual promoter pHW2000 plasmids containing each of the influenza A virus gene segments were used to transfect MDCK/293T cocultured cells. Virus stock was prepared by inoculation of 10-day-old embryonated chicken eggs. Viral RNA was isolated directly from allantoic fluid of inoculated eggs by using an RNA extraction kit (RNeasy; Qiagen). Reverse transcription-PCR of viral RNA used a universal primer set for influenza A virus (20), and subsequent sequencing was completed by the Hartwell Center for Bioinformatics and Biotechnology at St. Jude Children's Research Hospital. All experiments using reverse genetics viruses were undertaken in a U.S. Department of Agriculture-approved biosafety level 3+ containment facility. All assays utilizing recombinant viruses were undertaken in Vero cells infected at a multiplicity of infection of 3. Peak titers of reverse genetics viruses were determined by single-step growth analysis in MDCK cells. Cells were infected for 1 h and then washed with phosphate-buffered saline (PBS; pH 2.2) to remove free infectious virus particles. Cells were incubated at 37°C in minimal essential medium (containing 10% fetal bovine serum and 1% glutamine). Supernatants were collected 2, 4, 6, 8, and 10 h postinfection and stored at −70°C for titration.

Transient expression of HA proteins. Monolayers of Vero cells in six-well dishes (85 to 95% confluence) were transiently transfected with 1 μg of pCAGGS HA protein DNA by using a Lipofectamine Plus expression system (Invitrogen, Carlsbad, CA) according to the manufacturer's instructions. Transfected Vero cells were incubated for 4 h at 37°C. DMEM (containing 10% fetal bovine serum and 1% glutamine) was then added to cells, and cells were incubated for 16 h at 37°C. Cells were then treated as indicated for each experiment.

Adjustment of pH in vitro. The pH of phosphate-buffered saline with magnesium and calcium (PBS+) was adjusted by 0.1 M citric acid. Cell monolayers were exposed for 5 min at 37°C for syncytium formation and luciferase reporter gene assays and for 15 min at 37°C prior to processing for conformational flow cytometry.

Measurement of HA protein expression and cleavage by Western blotting, radioimmunoprecipitation, biotinylation, and flow cytometry. Sixteen hours after transfection, cell monolayers were washed twice with PBS+ solution. The samples were lysed with 0.5 ml of ice-cold radioimmunoprecipitation assay buffer containing Complete protease inhibitor cocktail (Roche, Indianapolis, IN). The lysate was spun at 67,000 × *g* in an Optima TLX ultracentrifuge (Beckman Coulter, Fullerton, CA). Cleared lysate was mixed with sample dye buffer containing 200 mM Tris, 8% sodium dodecyl sulfate (SDS), 0.2% bromophenol blue, 40% glycerol, and 12% β-mercaptoethanol. Samples were boiled for 5 min before being separated on 4–12% NuPAGE Bis-Tris polyacrylamide-SDS gels (Invitrogen). Proteins were transferred onto a polyvinylidene difluoride membrane, blocked with 5% fat-free milk, and probed by using rabbit polyclonal antisera against the peptide sequence (AADKESTQKAIDGVTNKVNSIIDK) in the HA2 subunit (Harlan Bioproducts for Science, Indianapolis, IN). Alexa Fluor 488-goat anti-rabbit conjugate secondary antibody was used to visualize bands with a Typhoon 9200 imager (GE Healthcare, Waukesha, WI). The band intensity was measured by using ImageQuant TL software (Molecular Dynamics, Sunnyvale, CA). Equal loading of wells was confirmed by Western blotting with a rabbit polyclonal primary antibody against the cellular protein GAPDH (glyceraldehyde-3-phosphate dehydrogenase; Abcam, Cambridge, MA). Radioimmunoprecipitation and biotinylation experiments were performed as described previously (28), using 25 μl of rabbit anti-HA2 peptide polyclonal primary antibody (1:200 dilution). Flow cytometry was performed as described previously (28), using the primary monoclonal antibody VN04-2 (1:500 dilution) (22), which reacts equally to both neutral- and low-pH conformations of the H5N1 HA protein (unpublished observation). Mean fluorescence intensity (MFI) values were normalized to those of the A/chicken/Vietnam/C58/04 wild-type HA protein. Monoclonal antibodies VN04-9 and VN04-16 (22) were used to measure the pH dependence of conformational changes of the HA protein at a 0.1 pH unit resolution. The pH of conformational changes was determined as the point at which 50% change in signal occurred between baseline and maximum.

Luciferase reporter gene assay for cell-cell membrane fusion. To quantify membrane fusion, we performed a luciferase reporter gene assay as described previously (33). Briefly, six-well dishes containing Vero cells (70 to 80% confluence) were transfected with 1.0 μg of luciferase control DNA (Promega, Madison, WI) and 1.0 μg of pCAGGS HA DNA. At 16 h posttransfection, BSR-T7/5 target cells (expressing T7 RNA polymerase) were overlaid onto the Vero cells expressing the HA protein (2). After a 1-h incubation at 37°C, the monolayers were washed and pH treated at a 0.2 pH unit resolution. Cells were neutralized by using DMEM (containing 10% fetal bovine serum and 1% glutamine) and left at 37°C for 6 h (21). Samples were lysed in reporter lysis buffer (Promega) and clarified by centrifugation at 15,000 × *g* in a tabletop centrifuge (5417C; Eppendorf, Germany) at room temperature. From each clarified lysate, a 150-μl sample was transferred to a 96-well plate (Lumitrac 200; Promega). The luciferase activity resulting from fusion of the two cell populations was quantified with a Veritas luminometer (Promega), using 50 μl of luciferase assay substrate (Promega) injected into each sample.

Syncytium assay for cell-cell fusion by HA mutants. Monolayers of BHK-21 cells grown in six-well plates were transfected with 1 μg of pCAGGS HA as described above. Monolayers of Vero cells grown in six-well plates were infected with recombinant virus at a multiplicity of infection of 3. At 16 h posttransfection or 6 h postinfection, cell monolayers were pH treated as described above at a 0.1 pH unit resolution. Cells were neutralized by using DMEM (containing 10% fetal bovine serum and 1% glutamine) and incubated at 37°C for 2 h. Samples were fixed and stained with Hema-3 Stat Pack staining kit (Fisher) according to the manufacturer's instructions. Representative fields were captured with a Nikon D70 digital camera attached to a Nikon Eclipse TS100 inverted microscope.

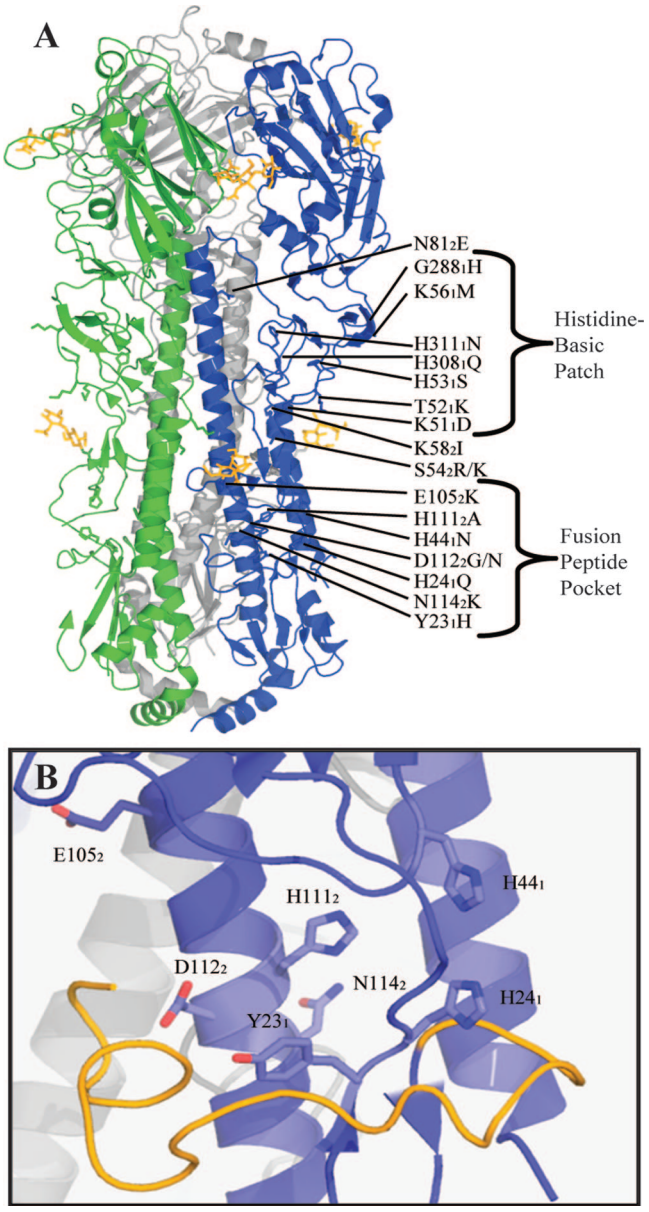

FIG. 1. (A) Locations of the 19 point mutations introduced into the HA protein of A/chicken/Vietnam/C58/04 (H5N1) influenza virus. Mutations are mapped to the available trimeric structure of the closely related A/Vietnam/1203/04 HA protein (42) (PDB:2fk0). (B) Fusion peptide (yellow) and fusion peptide pocket (blue). Residues mutated in the present study are shown with amino acid side chains. Subscript numbers denote the HA subunit in each mutation. H5 numbering is used throughout.

RESULTS

Selection of HA protein mutations. To identify amino acid residues that regulate the pH of activation of the HA protein of an H5N1 influenza virus, two sets of mutations were generated in the background of the HA protein of A/chicken/Vietnam/C58/2004 (H5N1) (Fig. 1). Eight mutations to HA2 coiled-coil residues that alter the pH of activation of H3 and H7 HA proteins were selected for the present study on the H5N1 HA protein (7, 39, 41, 49). Eleven mutations to introduce or remove basic residues were selected by sequence alignment of HA proteins from different subtypes. Y23$_1$H, K51$_1$D, G288$_1$H, and H308$_1$Q were selected based upon prevalence in the H1 HA protein; H44$_1$N, H53$_1$S, and H311$_1$N were selected based upon prevalence in the H3 HA protein; H111$_2$A was selected based upon prevalence in the H7 HA protein, and H24$_1$Q and K56$_1$M were selected based upon prevalence in the H9 HA protein. T52$_1$K was selected because it is one of the residues that differs between the A/chicken/Vietnam/C58/04 HA protein being studied, and the HA protein of A/Vietnam/1203/04 H5N1 virus being used as a structural model for comparison. This mutation is the only one that has been observed in circulating H5N1 influenza virus isolates.

Only the H111$_2$A mutation causes substantial changes in protein expression and cleavage. The effects of mutations on total HA protein expression were analyzed by radioimmunoprecipitation (15-min pulse and a 0-min chase) and Western blotting (Fig. 2). Densitometric analysis of HA0 band intensity showed that the initial expression of all mutant HA proteins was 64 to 125% that of the wild type (Fig. 2A and B and Table 1), showing that the mutations did not abrogate initial expression of the HA0 precursor protein.

In Western blot experiments, whole-cell lysates were collected 16 h posttransfection to determine the steady-state levels of expression and cleavage of the HA protein. SDS-polyacrylamide gel electrophoresis (PAGE) analysis showed that the HA protein containing an H111$_2$A mutation accumulated only as an HA0 precursor protein at a level 26% that of wild type; it was not detectable in the stable, cleaved form (Fig. 2C and Table 1). For the remaining 18 HA proteins containing mutations, the levels of cleavage were similar to that of the wild type, and the levels of expression were 42 to 186% that of the wild type (Fig. 2C and D and Table 1). A lower initial expression of the HA protein mutants G288$_1$H, H311$_1$N, and D112$_2$G, as measured by radioimmunoprecipitation, resulted in lower steady-state expression levels, as measured by Western blotting.

The effects of the mutations on the cell surface expression of HA proteins were studied by biotinylation and flow cytometry experiments. Intact cells were biotinylated 16 h posttransfection and analyzed by Western blotting. The levels of cleavage of all biotinylated HA proteins containing mutations were comparable to that of the wild type, except for the HA protein containing an H111$_2$A mutation (Fig. 3A and B and Table 1). Of the mutations in the histidine or basic patch, the H24$_1$Q, T52$_1$K, H53$_1$S, and H308$_1$Q mutations caused significant increases, and the G288$_1$H, H311$_1$N, and H111$_2$A mutations significant decreases in cell surface expression compared to the wild type. Of the HA2 coiled-coil mutations, the S54$_2$R, K58$_2$I, and D112$_2$N mutations resulted in significant increases, and the E105$_2$K and N114$_2$K mutations significant decreases in cell surface expression compared to the wild type.

In flow cytometry experiments, intact cells were labeled 16 h posttransfection with the anti-H5 HA protein monoclonal antibody VN04-2 (22), which binds with equal affinity to both neutral- and low-pH forms of the A/chicken/Vietnam/C58/2004 (H5N1) HA protein (data not shown). The surface expression levels of most HA proteins containing histidine or basic patch mutations were similar to those of the wild type, although the H111$_2$A mutation reduced the cell surface ex-

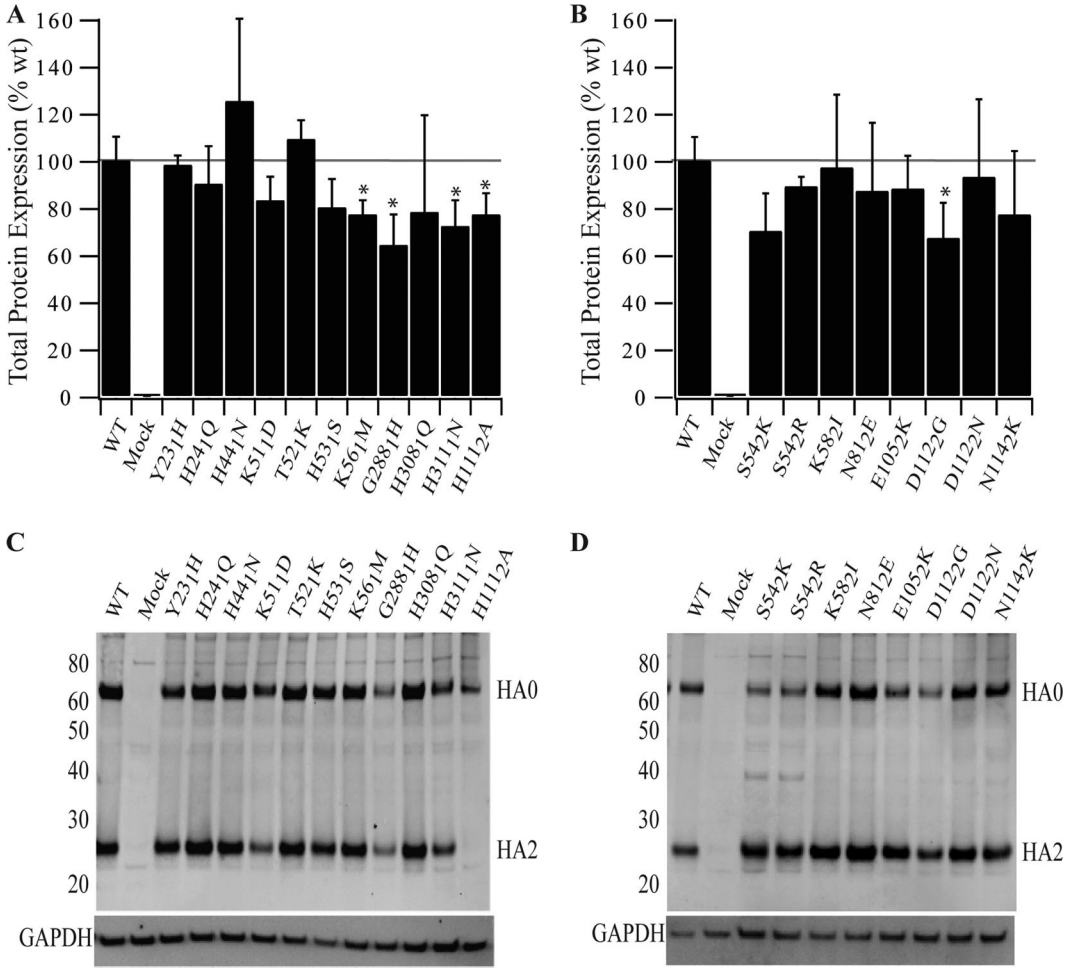

FIG. 2. Total expression of wild-type and mutant HA proteins in Vero cells. (A) Histidine or basic patch mutants; (B) HA2 coiled-coil mutants. Total initial expression was determined by immunoprecipitation analysis. At 16 h posttransfection, Vero cells expressing wild-type and mutant HA protein were serum starved for 30 min and subsequently labeled with [^{35}S]Promix for 15 min. HA0 expressed during the labeling pulse was immunoprecipitated by using the A0110 polyclonal antibody and analyzed by SDS-PAGE under reducing conditions. Initial expression was normalized to the wild-type HA protein. The horizontal line represents 100% expression. Error bars represent the standard deviation from triplicate experiments. Asterisks indicate a significant difference ($P < 0.05$) as determined by an independent group t test. (C and D) Total expression and cleavage of histidine or basic patch mutants (C) and HA2 coiled-coil mutants (D). Vero cells expressing wild-type and mutant HA proteins were processed 16 h posttransfection and analyzed by Western blotting with polyclonal antibody A0110 raised against a peptide motif in the HA2 subunit of H5 HA protein. Uncleaved HA0 precursor and the HA2 cleavage product are indicated. GAPDH loading controls are shown. WT, wild type.

pression of the HA protein to 31% that of the wild type (Fig. 3C and D and Table 1). Mutations in the HA2 coiled-coil region caused a more polarized effect. Both mutations at residue S54 resulted in increased cell surface expression. For the remaining HA2 coiled-coil mutations, cell surface expression levels were 62 to 92% compared to that of the wild type.

In general, cell surface expression levels from flow cytometry experiments were lower than those obtained by Western blot analyses of the biotinylated surface protein. Binding of the VN04-2 monoclonal antibody suggests that the HA proteins are correctly folded. However, we have yet to determine whether the VN04-2 antibody binds preferentially to either the cleaved or the uncleaved form of the HA protein or binds with equal affinity to both. The detection of some $H111_2A$ protein at the cell surface suggests that this antibody can recognize the uncleaved form of the HA protein. In contrast, the biotinylation analysis is expected to detect equally both uncleaved and cleaved forms of the HA protein at the cell surface but may not accurately measure the amount of functional protein at the cell surface (i.e., the protein competent for mediating membrane fusion). The collective results from both assays show that most mutant HA proteins were expressed at the cell surface of transfected cells at levels comparable to that of wild-type C58 HA protein. Moreover, except for $H111_2A$, the levels of cleavage of all other mutant HA proteins were similar to that of the wild type (Fig. 4 and Table 1). Levels of cleavage of surface expressed protein could be increased by ca. 11% with the presence of 5 μg of exogenous trypsin/ml for 30 min at 37°C (data not shown), suggesting that a population of HA protein reaches the cell surface uncleaved.

Five individual mutations to the HA protein change the pH of membrane fusion. The extents to which the wild-type and mutant HA proteins promote cell-to-cell membrane fusion were measured as a function of pH by syncytium and luciferase

TABLE 1. Phenotypes of wild-type and mutant influenza A HA proteins[a]

H5 numbering	H3 numbering	Total protein expression		Surface expression		Cleavage		pH of fusion		pH of conformation change	
		IP[b] (mean ± SD)	Western blot	MFI[c] (mean ± SD)	Biotinylation[d] (mean ± SE)	Total[e]	Surface[f] (mean ± SE)	Syncytia[g]	Luciferase[h]	VN04-9[i]	VN04-16[j]
Wild type		100 ± 10	100	100 ± 13	100 ± 23	0.45	0.55 ± 0.04	5.5	5.5	5.5	5.4
$Y23_1H$	$Y17_1H$	98 ± 4	72	95 ± 11	128 ± 16	0.49	0.60 ± 0.00	+0.4	+0.4	+0.3	+0.4
$H24_1Q$	$H18_1Q$	90 ± 16	96	91 ± 18	188 ± 41	0.48	0.49 ± 0.01	–0.3	–0.3	–0.4	–0.4
$H44_1N$	$H38_1N$	125 ± 35	91	88 ± 9	113 ± 21	0.49	0.60 ± 0.01	–0.1	0.0		
$K51_1D$	$K45_1D$	83 ± 10	55	95 ± 5	85 ± 14	0.41	0.69 ± 0.03	0.0	–0.1		–0.1
$T52_1K$	$T46_1K$	109 ± 8	104	98 ± 10	165 ± 19	0.45	0.56 ± 0.02	0.0	0.0		
$H53_1S$	$H47_1S$	80 ± 12	83	88 ± 5	146 ± 28	0.45	0.60 ± 0.02	0.0	0.0		0.0
$K56_1M$	$K50_1M$	77 ± 6	124	94 ± 4	134 ± 28	0.48	0.55 ± 0.05	0.0	–0.1		
$G288_1H$	$G275_1H$	64 ± 13	42	98 ± 6	52 ± 16	0.44	0.72 ± 0.02	0.0	–0.1		
$H308_1Q$	$H295_1Q$	78 ± 41	121	107 ± 8	166 ± 14	0.44	0.47 ± 0.07	0.0	–0.2		
$H311_1N$	$H298_1N$	72 ± 11	59	81 ± 4	32 ± 13	0.43	0.69 ± 0.02	0.0	0.0		
$H111_2A$	$H111_2A$	77 ± 9	26	31 ± 1	16 ± 4	0.07	0.10 ± 0.02	NA	NA		
$S54_2K$	$S54_2K$	70 ± 16	78	151 ± 20	113 ± 40	0.64	0.60 ± 0.07	0.0	0.0		
$S54_2R$	$S54_2R$	89 ± 4	91	138 ± 10	159 ± 52	0.61	0.54 ± 0.04	0.0	0.0		
$K58_2I$	$K58_2I$	97 ± 31	167	86 ± 10	136 ± 5	0.57	0.61 ± 0.02	–0.4	–0.4	–0.4	–0.4
$N81_2E$	$N81_2E$	87 ± 29	186	92 ± 7	103 ± 7	0.56	0.52 ± 0.04	0.0	–0.1		
$E105_2K$	$E105_2K$	88 ± 14	117	72 ± 10	70 ± 11	0.61	0.65 ± 0.04	–0.3	–0.2	–0.1	–0.2
$D112_2G$	$D112_2G$	67 ± 15	74	62 ± 8	96 ± 13	0.61	0.53 ± 0.05	0.0	0.0	+0.3	+0.3
$D112_2N$	$D112_2N$	93 ± 33	135	84 ± 10	150 ± 32	0.54	0.43 ± 0.06	0.0	+0.1	+0.2	+0.3
$N114_2K$	$N114_2K$	77 ± 27	108	78 ± 6	43 ± 11	0.49	0.43 ± 0.11	+0.2	+0.3	+0.5	+0.5

[a] Influenza A virus HA proteins expressed from pCAGGS DNA in Vero cells.
[b] Total HA0 expression after 15 min of [^{35}S]methionine pulse-labeling. Data are normalized to wild-type HA protein. IP, immunoprecipitation.
[c] Cell surface expression (expressed as the MFI) was determined by flow cytometry using monoclonal antibody VN04-2. Data are normalized to wild-type C58 HA protein. The reported error indicates the standard deviation from triplicate experiments.
[d] Cell surface expression determined by biotinylation. Data are normalized to wild-type C58 HA protein. The reported error indicates standard error from triplicate experiments.
[e] That is, the cleavage ratio of total cell lysates determined using the formula HA2/(HA0 + HA2).
[f] That is, the cleavage ratio determined by biotinylation. Data are normalized to the wild-type C58 HA protein. The reported error indicates standard error from triplicate experiments.
[g] A syncytium formation assay for the pH of membrane fusion was determined as the last pH point at which syncytium formation was within a representative field of view. NA, absence of syncytium formation.
[h] pH of membrane fusion derived from the luciferase reporter gene assay was determined as the point at which 50% of maximum increase in signal was achieved. NA, absence of fusion as determined by this assay.
[i] Monoclonal antibody VN04-9 favors the metastable conformation of the H5 HA protein. The pH of conformational change was determined as the pH at which a 50% decrease in signal was observed between baseline and maximum.
[j] Monoclonal antibody VN04-16 favors the low-pH conformation of the H5 HA protein. The pH of conformational change was determined as the pH at which a 50% increase in signal was observed between baseline and maximum.

reporter gene assays. Syncytium formation between BHK-21 cells was initiated 16 h posttransfection, and the pH of fusion was defined as the highest pH at which syncytium formation was observed (Fig. 5 and Table 1). The wild-type C58 HA protein promoted syncytium formation at pH 5.5. Eight of the eleven mutations in the histidine or basic patch caused a pH change of 0.1 U or less. The $Y23_1H$ mutation increased the pH of syncytium formation by 0.4 pH units, whereas the $H24_1Q$ mutation decreased it by 0.3 pH units. The $H111_2A$ mutant showed no syncytium formation at any pH over the range measured (pH 5.0 to 6.0), a finding consistent with this mutant not being present on the cell surface of transfected cells in a cleaved form. Five of the eight mutations in the HA2 coiled-coil group caused no change in the pH of syncytium formation. The $K58_2I$ and $E105_2K$ mutations decreased the pH of fusion by 0.4 and 0.2 pH units, respectively, whereas the $N114_2K$ mutation caused a pH increase of 0.2 pH units.

A luciferase reporter gene assay was also used to measure the effects of the mutations on the pH of HA-mediated membrane fusion (Table 1 and Fig. 6A and B). Similar to results from the syncytium assays, in the luciferase assay the $Y23_1H$ mutation increased the pH of fusion by 0.4 U, the $H24_1Q$ mutation decreased the pH by 0.3 U, the $H111_2A$ mutation eliminated membrane fusion, and the remaining eight mutations in the histidine or basic group had little effect on the pH of luciferase activity (Table 1). The $K58_2I$, $E105_2K$, and $N114_2K$ mutations in the HA2 coiled-coil group also caused similar shifts in the pH of membrane fusion in both the syncytium and the luciferase assays, and the remaining five HA2 mutations had little or no effect on the pH of acid stability of the C58 H5 HA protein. Unexpectedly, the mutations $D112_2G$ and $D112_2N$ did not increase the pH of membrane fusion of the H5 HA protein in either assay, despite substantially altering the pH of fusion in H3 and H7 subtypes (7, 39, 49). This assay was also used to measure the fusogenic efficiency of the mutants compared to the wild type. It showed that the majority of mutants had no significant effect on the proportion of cells fused under conditions of low pH (Fig. 6C and D). Mutants $K51_1D$ and $H53_1S$ had caused a significant change in fusogenic efficiency, similar to what has previously been hypothesized for basic residues in this region for H1 and H5 subtypes (42, 43). $E105_2K$ decreased the fusogenic potential of the HA protein, while $H111_2A$ demonstrated a very low level of fusion consistent with observations made in the syncytium formation assay. The very low signal demonstrated for the $H111_2A$

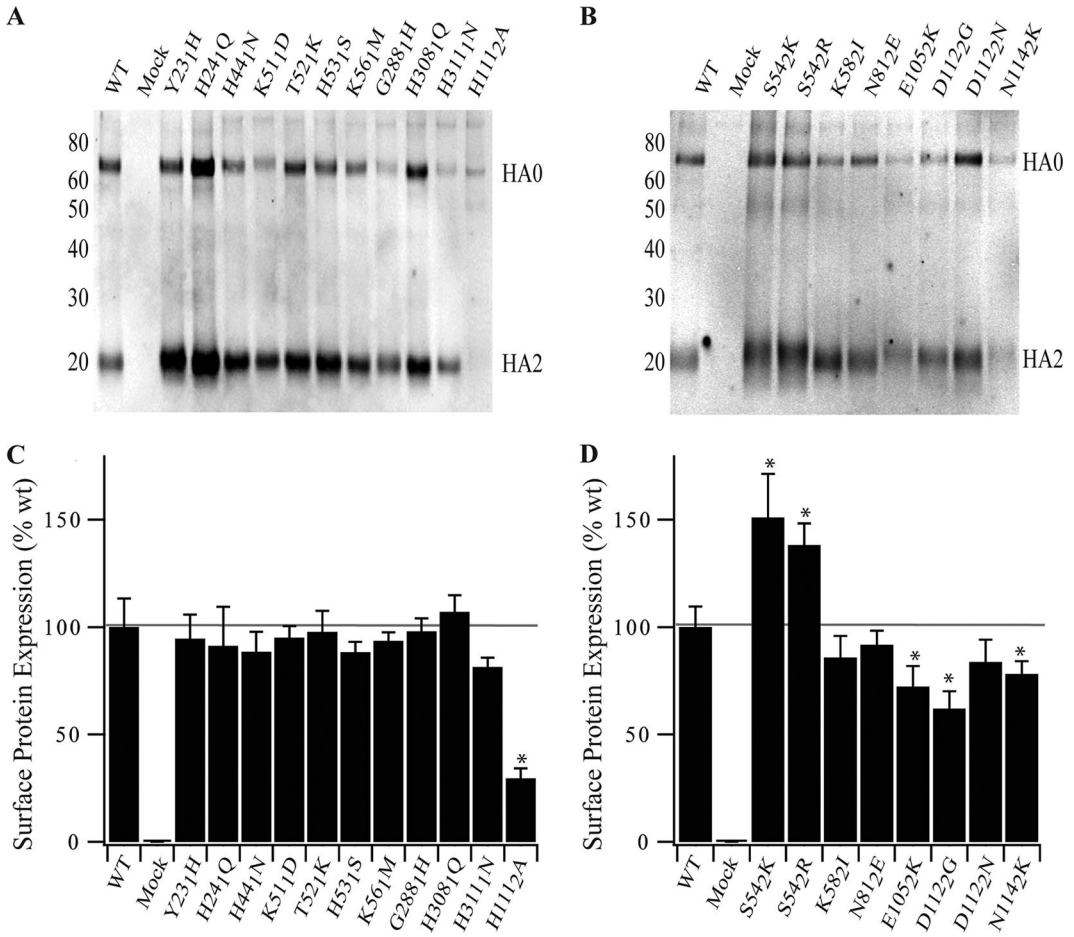

FIG. 3. Cell surface expression of wild-type and mutant HA proteins as determined by surface protein biotinylation assay. (A) Histidine or basic patch mutants; (B) HA2 coiled-coil mutants. Vero cells expressing wild-type or mutant HA protein were biotinylated for 30 min. The biotinylated protein was isolated by using streptavidin-conjugated Sepharose beads, analyzed by SDS-PAGE under reducing conditions, and subsequently analyzed by Western blotting. Western blotting with polyclonal antisera A0110 against a peptide sequence in HA2 shows the uncleaved HA0 precursor and the HA2 subunit cleavage product (indicated). (C and D) Surface expression of H5 HA protein using monoclonal antibody VN04-2 for histidine or basic patch mutants (C) and HA2 coiled-coil mutants (D) (22). MFI values were normalized to 100% surface expression for wild-type C58 HA protein. The horizontal line represents 100% expression. Error bars represent the standard deviation from triplicate experiments. Asterisks indicate a significant difference ($P < 0.05$), as determined by an independent group t test. WT, wild type.

mutant is consistent with the syncytium formation assay showing no syncytium formation for this mutant at any pH.

Mutations that alter the pH of membrane fusion also alter the pH of HA protein conformational changes. The influenza A virus HA protein is expressed on the surfaces of infected cells and virions in a metastable, spring-loaded conformation and undergoes a dramatic, pH-dependent molecular rearrangement that promotes membrane fusion (10, 37). To determine whether the histidine or basic patch mutations $Y23_1H$, $H24_1Q$, $K51_1D$, and $H53_1S$ and the HA2 coiled-coil mutations $K58_2I$, $E105_2K$, $D112_2G$, $D112_2N$, and $N114_2K$ change the pH of refolding of the HA protein, flow cytometry experiments were performed with conformation-based monoclonal antibodies (Fig. 7 and Table 1). The monoclonal antibodies VN04-9 and VN04-16 (22) bound preferentially to the native and low-pH conformations, respectively, of the wild-type HA protein of A/chicken/Vietnam/C58/04 (H5N1) (Fig. 7A and B). On the basis of these differences in binding preference, the pH dependence of conformational changes in the HA protein was determined by flow cytometry. Unexpectedly, the pH of conformational changes for $D112_2G$ and $D112_2N$ were 0.3 and 0.25 pH units higher, respectively, than the pH of the membrane fusion. Similarly, the $N114_2K$ mutation induced conformational changes at a pH ~0.3 U higher than its pH of membrane fusion. It is possible that the HA proteins containing $D112_2G$, $D112_2N$, or $N114_2K$ mutations undergo somewhat localized changes in conformation detected by the antibodies at a pH higher than that required to trigger the complete HA protein refolding necessary to promote membrane fusion. In contrast, the HA proteins containing mutations $Y23_1H$, $H24_1Q$, $K58_2I$, and $E105_2K$ showed shifts in the pH of conformational changes similar to those observed in the syncytia and luciferase assays (Fig. 7C and Table 1). Analysis of $K51_1D$ and $H53_1S$ with VN04-16 also confirmed that the pH of conformational change matched the findings of the pH of membrane fusion assays (Table 1).

Mutations that alter the pH of fusion in transfected cells have a conserved effect in reverse genetics virus. In order to

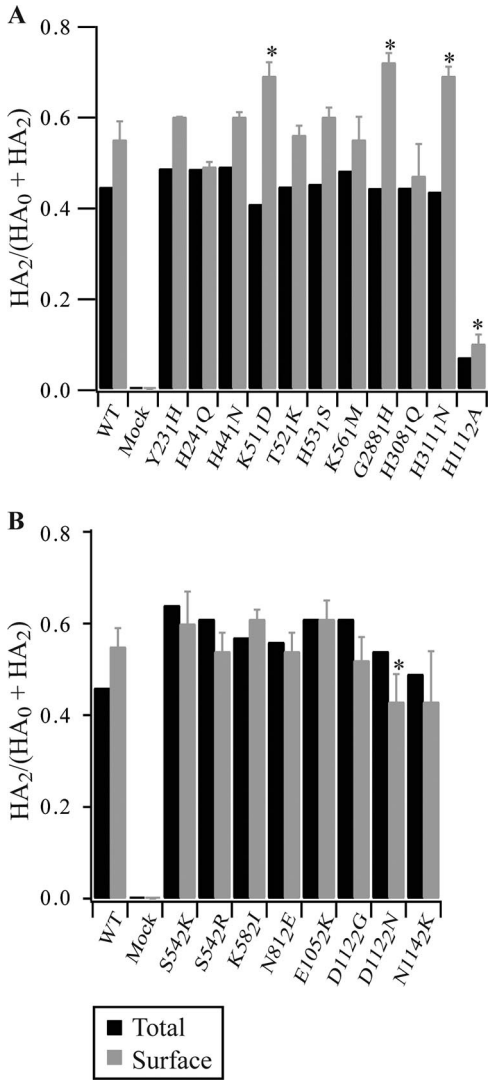

FIG. 4. Cleavage of wild-type and mutant H5 HA proteins. Intensities of the HA0 and HA2 bands from Fig. 2C and D were quantified, and the fraction of cleaved HA2 was calculated by dividing HA2 by total HA (represented by HA0 + HA2, since the HA1 protein is not observed in the assay). Error bars represent standard errors from three separate experiments. Asterisks indicate a significant ($P < 0.05$) difference as determined by an independent group *t* test. WT, wild type.

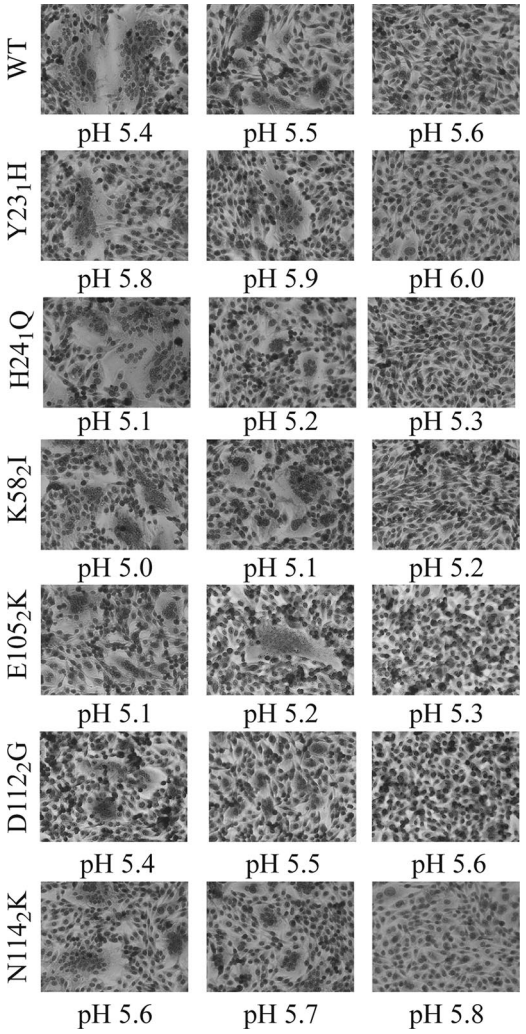

FIG. 5. Representative micrographs of the syncytium formation assay to observe the pH of membrane fusion for wild-type (WT) and mutant C58 HA proteins. The micrographs show the presence or absence of syncytium formation when BHK-21 cells expressing HA protein were incubated at the indicated pH. The pH of fusion was measured as the highest pH value at which syncytium formation was observed.

determine whether changes in the pH of fusion observed in the transient-transfection system were applicable to H5N1 recombinant virus, wild-type A/chicken/Vietnam/C58/04 virus, and viruses containing the mutations Y23$_1$H, H24$_1$Q, K58$_2$I, and N114$_2$K in the HA gene were generated by using the eight-plasmid system (19). These four mutations were selected because they gave a range of changes in the pH of fusion encompassing a 0.8 pH unit range around the value observed for wild-type HA protein. All viruses were successfully rescued, and sequencing determined that only the mutation of interest was present in each case. Single-step growth analysis using the viruses showed that the peak titers obtained were analogous for all viruses tested. Furthermore, the expression and cleavage of virus-derived HA protein was confirmed by Western blotting of virus-infected Vero cells. The pH of fusion for each virus was determined by using a syncytium formation assay in Vero cells. Table 2 shows that mutant and wild-type HA proteins were successfully expressed and cleaved in virus-infected cells. Furthermore, the shift in the pH of fusion is similar to that observed in transfected cells. The pH of fusion for N114$_2$K was closer to the value of pH of conformational change observed in transfected cells.

DISCUSSION

We have investigated how the pH of activation of the H5N1 HA protein is regulated by introducing 19 individual amino acid mutations into the HA protein of A/chicken/Vietnam/C58/04 (H5N1). We then characterized the mutational effects on expression, cleavage, conformational changes, and membrane fusion of the HA protein. Seven of the mutations were

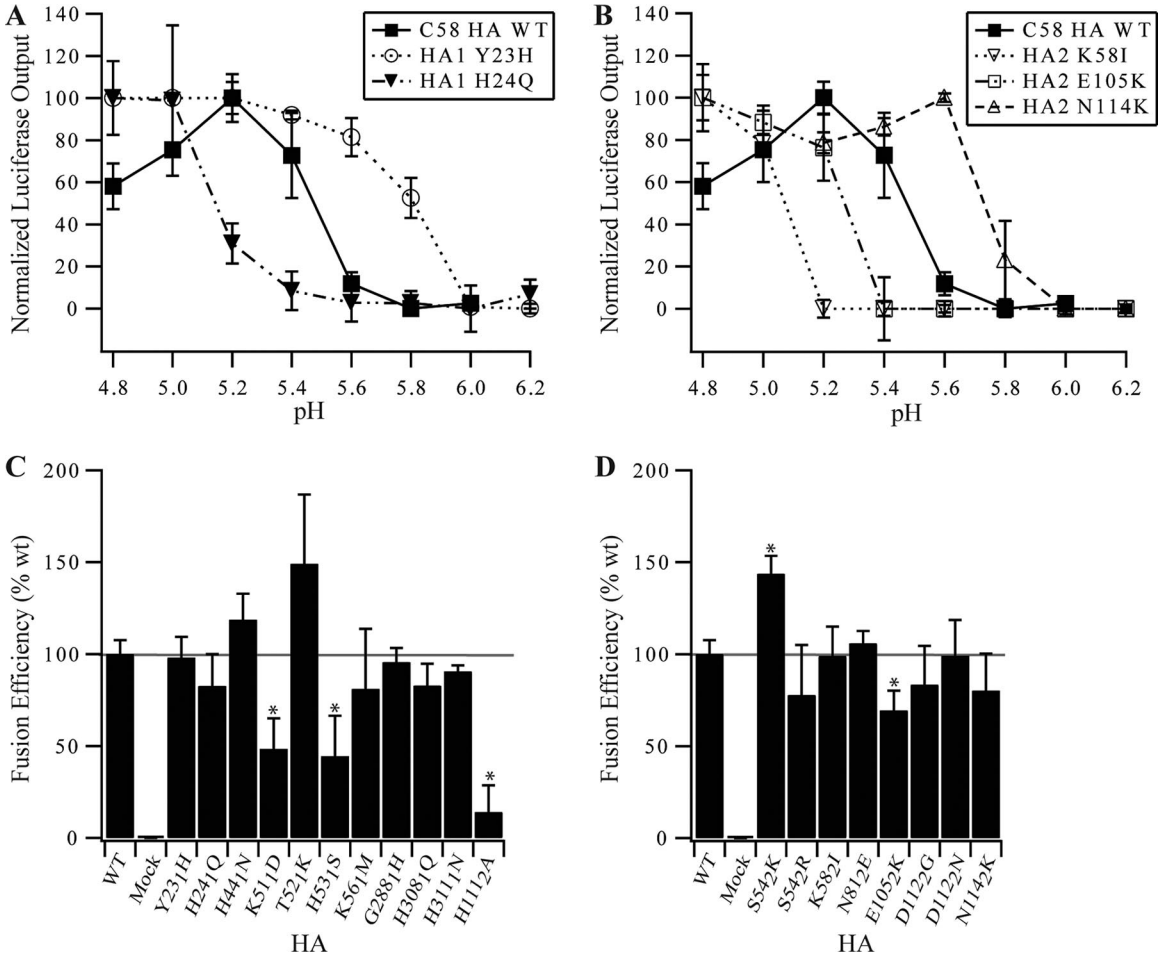

FIG. 6. Luciferase membrane fusion assay to measure the pH of fusion of H5 HA proteins. Vero cells were cotransfected with pCAGGS HA plasmids and T7 control DNA. At 16 h posttransfection, Vero effector cells were overlaid with BSR-T7/5 cells that express T7 polymerase (2). The two cell populations were then exposed to low-pH buffer conditions and coincubated for 6 h to allow cell-to-cell fusion to occur. The extent of membrane fusion was measured as the difference in signal between mock-transfected cells (T7 control DNA only) and the maximum signal acquired for the wild-type HA protein. The pH of fusion was determined as the point at which a 50% change in signal occurred. Error bars represent the standard deviation from triplicate experiments. Examples are shown for histidine or basic patch mutants (A) and HA2 coiled-coil mutants (B). (C and D) Comparative efficiency of fusion between mutant and wild-type HA proteins. Asterisks indicate a significant difference ($P < 0.05$) as determined by an independent group t test.

found to alter the pH of membrane fusion and/or protein refolding by ~0.2 pH units or more. Six of the mutations are located in the fusion peptide pocket, and the $K58_2I$ mutation is located in the "A" α-helix that buttresses the central HA2 coiled coil in the metastable structure (Fig. 1). An $H111_2A$ mutation in the fusion peptide pocket significantly decreased expression of the HA protein and completely eliminated cleavage and membrane fusion. Eleven other mutations had little effect on the pH of fusion of the H5N1 HA protein, including all of the mutations to residues in a membrane-distal histidine or basic patch at the interface of the HA1 and HA2 domains (Fig. 1). Four mutants capable of altering the pH of fusion in transfected cells were introduced into reverse genetics virus. All viruses were successfully rescued and demonstrated a shift in pH of fusion similar to that observed in transfected cells expressing mutant HA proteins.

Residues in the fusion peptide pocket may universally regulate HA acid stability across all HA subtypes. Consistent with our findings for the H5 HA protein, previous studies have shown that residues in the fusion peptide pocket regulate the acid stabilities of H3 and H7 HA proteins (7, 16, 35, 39–41, 46). For example, the $Y23_1H$ mutation in the H5 HA protein in our study increased the pH of activation by 0.4 pH units. The reverse mutation in the H3 HA protein $H17_1Y$ (H3 numbering) has the opposite effect of decreasing the pH of activation by 0.3 pH units (46).

High-resolution structures have been determined for HA proteins of A/Vietnam/1194/04 (H5N1) and A/Vietnam/1203/04 (H5N1) viruses, which differ from the HA protein of A/chicken/Vietnam/C58/04 (H5N1) by only four and five amino acids, respectively (42, 52). In the high-resolution structures of the H5 HA protein, the $Y23_1$ residue is nearly completely buried by the fusion peptide after cleavage, and the hydroxyl group of the $Y23_1$ side chain forms a hydrogen bond with the backbone amine of fusion peptide residue $G13_2$ (Fig. 8A). An $Y23_1H$ mutation may destabilize the H5 HA protein

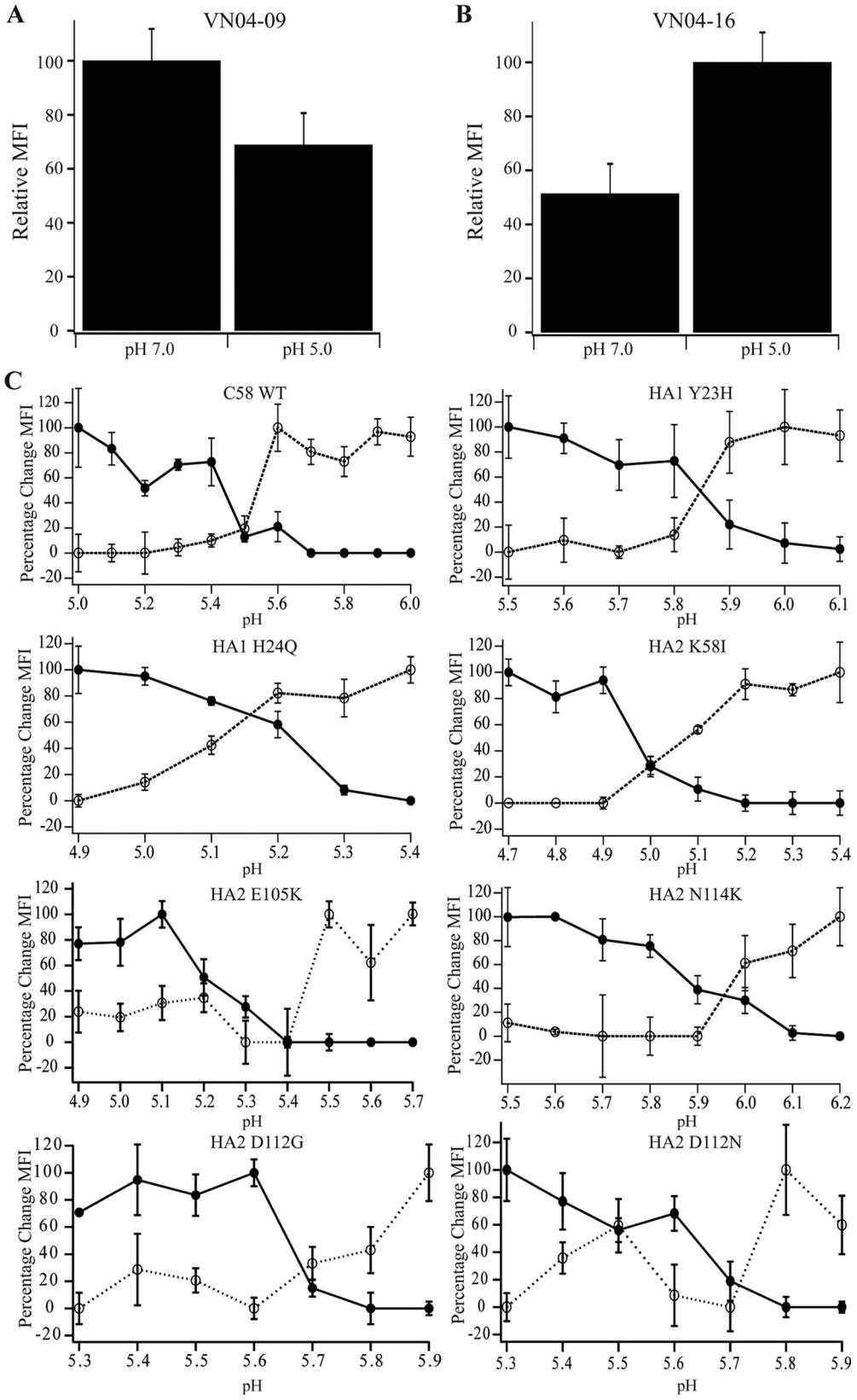

FIG. 7. Analysis of the pH of conformational changes by flow cytometry using monoclonal antibodies that bind preferentially to either the neutral or low-pH forms of the H5N1 HA protein. Vero cells were transfected with pCAGGS HA plasmids. At 16 h posttransfection, cells were stained and analyzed by flow cytometry. (A) Monoclonal antibody VN04-9 binding profile at neutral (7.0) and low (5.0) pH. (B) Monoclonal antibody VN04-16 binding profile at neutral (7.0) and low (5.0) pH. (C) Conformational change of wild-type and mutant HA proteins as characterized by the change in monoclonal antibody binding. The pH of the conformational change was determined as the point at which a 50% change in signal between maximum and baseline was observed. Dotted traces with open circles denote binding of VN04-9, and solid traces with filled circles show VN04-16 monoclonal antibody binding. The MFI was measured by flow cytometry.

TABLE 2. Initial characterization of mutant and wild-type rescued viruses

Virus	Mean ± SD			ΔpH[d]
	Peak titer[a]	Expression[b]	Cleavage[c]	
Wild type	6.03 ± 0.66	100 ± 1	0.66 ± 0.05	
$Y23_1H$	5.83 ± 0.25	103 ± 6	0.57 ± 0.04	0.4
$H24_1Q$	5.77 ± 0.47	98 ± 4	0.61 ± 0.09	−0.3
$K58_2I$	5.86 ± 0.28	98 ± 20	0.64 ± 0.09	−0.6
$N114_2K$	5.59 ± 0.24	99 ± 3	0.48 ± 0.06	0.5

[a] The peak titer determined by a single-step growth curve 12 h postinfection at multiplicity of infection of 3. Titers expressed as $\log_{10}$ PFU/ml.
[b] Expression was determined by Western blotting of whole-cell lysates of infected cells. The results represent the total number of HA0+HA2 bands as detected by A0110 polyclonal antibody. Expression data were normalized to the value for wild-type C58 HA protein.
[c] The cleavage ratio of total cell lysates was determined by using the formula HA2/(HA0 + HA2).
[d] The change in pH of fusion (ΔpH) was determined by syncytium formation assay.

by a loss of this important hydrogen bonding interaction between the fusion peptide and its pocket. A comparison of H5 and H3 HA structures shows that the fusion peptide and fusion peptide pocket residues adopt similar conformations in both subtypes, thus allowing for similar interactions in both subtypes (Fig. 8). Therefore, the $H17_1Y$ mutation may stabilize the H3 HA protein by introducing energetically favorable hydrogen bonding between residue 17 in the fusion peptide pocket and the fusion peptide. In fact, a molecular model of tyrosine at position 17 in the H3 HA protein and a comparison with H1 HA protein structures containing native tyrosine residues at position 17 are consistent with the hydroxyl group on the tyrosine side chain interacting with residues 10 and 12 of the fusion peptide in the context of the H3 HA protein (46). In the H3 HA structure, the native histidine at HA1 position 17 forms hydrogen bonds with the fusion peptide via water molecules. Although the analogous $Y23_1H$ residue in the H5 HA protein may also form similar hydrogen bonds with the fusion peptide via water molecules, the observation that this mutation makes the HA protein less acid stable is consistent with such potential interactions being weaker than direct interactions between the native tyrosine residue at position 23 in H5 HA1 subunit. Further evidence that H3 HA residue 17 (H5 HA residue 23) plays a critical role in activating the HA protein for membrane fusion is supported by the observations that mutation of H3 HA protein residue $H17_1$ to alanine, arginine, or glutamine increases the pH of membrane fusion by 0.4, 0.7, and 0.9 pH units, respectively (7, 39, 46, 50). On the basis of similarities between the H3 and H5 HA proteins in this region, $Y23_1A$, $Y23_1R$, and $Y23_1Q$ mutations in H5 are expected to destabilize the HA protein to a greater extent than the $Y23_1H$ mutation characterized here; however, such mutational analyses have not yet been performed.

HA2 residue 111 is also located in the fusion peptide pocket and is conserved along structural group-specific lineages (16, 35). For the H5 HA protein, an $H111_2A$ mutation decreased its expression, eliminated HA0 precursor cleavage, and blocked membrane fusion. Similar to the H5 HA protein, the H2 HA protein is also in the H1 structural clade and contains a histidine at HA2 residue 111. For the H2 HA protein, an $H111_2A$ mutation also eliminates its cell surface expression (46). The H3 HA protein belongs to a distinct structural lineage (H3 lineage) and contains a threonine residue at HA2 residue 111. For the H3 HA protein, a $T111_2A$ mutation has little effect on acid stability and fusogenicity, and $T111_2H$ and $T111_2V$ mutations increase the pH of activation and membrane fusion by 0.6 and 0.3 pH units, respectively (46).

The H3 and H7 structural clades contain a glutamate residue at HA2 residue 114 in the fusion peptide pocket, whereas the H1 structural clade (that includes the H5 HA protein) and the H9 structural clade contain an asparagine at HA2 residue 114. Despite clade-specific differences in wild-type residues at this position, mutation of HA2 residue 114 to a lysine residue in the H3, H7, and H5 HA proteins appears to cause in increase in the pH of conformational changes for all proteins by ~0.5 pH units (7). Although the overall effects of this mutation on acid stability are similar across the HA structural clades, the localized interactions that contribute to acid stability of the HA protein may differ for H5. Although the $N114_2$ residue of the H5 HA protein interacts with the hydroxyl group of tyrosine 22 of the fusion peptide, the $E114_2$ side chain of the H3 HA protein is twisted nearly 180° to interact with glutamine 47 of the HA2 subunit. The similar destabilization of H3, H5, and H7 HA proteins by a lysine mutation at HA2 residue 114 may

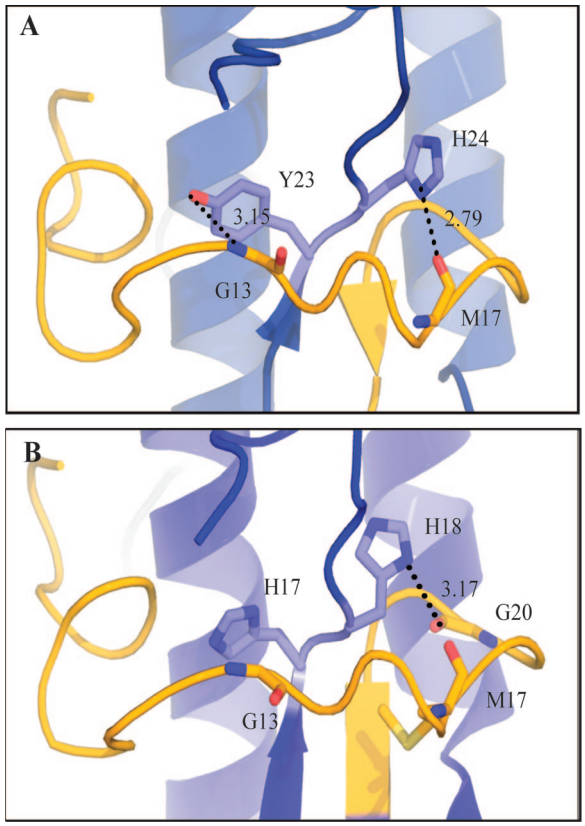

FIG. 8. Structural comparison of $Y23_1/H24_1$ residues in the H5 HA protein and the equivalent residues $H17_1/H18_1$ in the H3 HA protein. The HA1 subunit backbone is blue, and HA2 subunit fusion peptide backbone is yellow. Predicted bonding interactions are denoted by dashed lines with predicted bond lengths (in angstroms) given. Numbering in each diagram reflects that of the specific subtype in each case. (A) H5 HA protein using PDB:2fk0 (42); (B) H3 HA protein using PDB:1mql (17).

be due to steric hindrance or electrostatic disruptions, or both, of similar energetic magnitude in different local structural contexts.

In the H3 and H7 HA proteins, $D112_2G$ or $D112_2N$ mutations increase the pH of fusion by 0.4 and 0.35 pH units, respectively (7, 49). Mutation of $D112_2$ in the present study to either a glycine or asparagine residue increased the pH of conformational changes by ~0.3 pH units. However, both mutations caused membrane fusion at a pH similar to that for the wild-type C58 HA protein. An important role for HA2 residue D112 in regulating HA protein activation is consistent with its universal conservation across all known HA subtypes and selection on multiple occasions for H3 and H7 influenza viruses in the presence of drugs that elevate endosomal pH (7, 39, 46). A high-resolution structure of the H3 HA protein containing a $D112_2G$ mutation shows that a water molecule partially replaces the aspartate side chain, the mutation does not cause changes in the surrounding structure, and the mutation results in the loss of four intrachain hydrogen bonds with the fusion peptide (49). The data in our study suggest that the putative loss of similar intrachain hydrogen bonds in the H5 HA protein is not sufficient to destabilize the metastable conformation and trigger full membrane fusion. Previous studies of acid inactivation of H1, H2, and H3 HA proteins have provided evidence for conformational intermediates of the HA protein that undergo changes in tertiary structure but remain capable of fusion at low pH (25). This might be possible if the conformational intermediate involves limited movement of the HA1 subunit, which in turn facilitates release of the fusion peptide from its buried location (30). All monoclonal antibodies used for conformational flow cytometry had epitopes within the HA1 subunit (22). Therefore, discrepancies between the pH of conformational change and the pH of membrane fusion may reflect a transition between two structurally distinct metastable forms of the protein. Equally, the pH pulse used for the conformational flow cytometry was extended from 5 to 15 min. It has previously been shown that certain transitions of the HA protein conformational change are pH reversible (4) and that mutations in the HA can affect fusion kinetics (29). Therefore, the differences observed between the pH of conformational change and the pH of fusion assays may represent a change in fusion kinetics as a result of changes in the rate of transition between conformational intermediates of fusion, all of which are required for full fusion to occur. Further work would have to be undertaken to resolve the mechanisms involved in this process.

Not all mutations had similar effects on the acid stability of the HA protein for the H5, H3, and H7 subtypes. In fact, the mutation of residue 105 in HA2 to lysine had opposite effects on the acid stabilities of H5 and H3 HA proteins, most likely due to subtype-specific differences in sequence and interactions at this position. H3, H7, and H9 structural clades have a glutamine residue at position 105 of HA2, whereas H1 and H5 structural clades have a glutamate at this position. Moreover, a $Q105_2K$ mutation increases the pH of activation of the H3 HA protein by 0.3 pH units (7), whereas our study shows that an $E105_2K$ mutation decreases the pH of activation of the H5 HA protein by ~0.2 pH units. In the H3 HA protein structure (17), the glutamine side chain forms hydrogen bonds with the backbone amide of HA1 residue 29 and with the aspartate side chain of HA2 residue 109 by a water molecule and has van der Waals contact with the histidine side chain of HA2 residue 106 from an adjacent monomer. The loss of such energetically favorable interactions because of a mutation to a lysine residue may explain why this mutation increases the pH of activation of the H3 HA protein. A $Q105_2R$ mutation also increases the pH of activation of the H3 HA protein by 0.3 pH units, whereas $Q105_2A$ and $Q105_2E$ mutations have less pronounced effects (46). In the H5N1 HA protein structures (42, 52), the glutamate side chain at position 105 in HA2 does not have stabilizing interactions that are as extensive but may have electrostatic repulsion between residues $E105_2$ and $D109_2$. The reversal of side chain charge due to an $E105_2K$ mutation may increase the acid stability of the H5 HA protein by introducing electrostatic attraction between residue 105 and 109 in HA2.

The introduction of $Y23_1H$, $H24_1Q$, $K58_2I$, and $N114_2K$ mutations into the HA proteins of reverse genetics virus was tolerated. Examination of the pH of fusion for the mutant and wild-type viruses confirmed that the magnitude and direction of changes in the pH of fusion observed in cells expressing HA expressed as a result of transient transfection was similar to that observed in cells that had been infected with virus. Expression and cleavage of the mutant HA proteins was similar to that observed in the wild-type virus, suggesting that these shifts in pH of fusion were not a result of changes in either of these traits. Furthermore, the mutant viruses were able to replicate over a single cycle to titers analogous to wild-type virus. These observations underscore that the mutant viruses were capable of virus entry, membrane fusion, protein expression, cleavage, assembly, and budding over a single cycle of replication, despite demonstrating an altered pH of fusion. Although the mutations used in the present study represent changes between subtype, and not those present in isolated H5N1 influenza viruses, further characterization of these viruses will provide a model for the contribution of the pH of fusion to the phenotype of the virus with respect to transmissibility, host adaptation, and pathogenesis.

In summary, we have found that residues in the fusion peptide pocket play an important role in regulating the pH of activation of the HA protein from an H5N1 influenza A virus. Residues in other regions of the H5 HA molecule, such as K58 in HA2, can also regulate its acid stability. A comparison of our data on the H5 HA protein to previously reported findings on the H3 and H7 HA proteins shows that residues regulating acid stability are subtype specific and depend on local structure and interactions that occur between noncovalent bonding partners within this local structure. In cases where the orientation of local structural elements is similar between subtypes or strains, some mutations, such as at position 17 of HA1 (H3 numbering) and position 58 of HA2 (46), have similar effects on acid stability of the HA protein. However, in cases where the local structure may differ between strains or subtypes, the relative contribution of similar mutations to HA protein acid stability may differ, as seen for residue 105 in the HA2 subunit. When four residues capable of changing the pH of fusion were introduced into reverse genetics virus, they had a conserved effect on the pH of fusion with respect to the virus, while not having any substantial effects on initial virus growth or protein expression.

A potential role for changes in the acid stability of the HA

protein in the adaptation of influenza A viruses to different species has already been established for H3N2 and H7N3 viruses (15, 27). The importance of the HA protein in virus pathogenesis and host range has also been established. The presence of a polybasic cleavage site within H5 and H7 HA proteins results in intracellular cleavage by ubiquitous proteases and leads to systemic infection and greater pathogenicity in vivo (12, 32, 47). Changes in the receptor binding specificity of the HA1 subunit also alter the host range and cell tropism of influenza A viruses (18, 38). In our study, two mutations ($Y23_1H$ and $N114_2K$) increased the pH of activation of individually expressed H5 HA proteins in vitro and three mutations ($H24_1Q$, $K58_2I$, and $E105_2K$) decreased the pH of activation. The contribution of the pH of fusion to influenza virus phenotype has yet to be fully determined. However, the stability of the HA protein may contribute to the longevity of the virus in the environment (1) and therefore the ease with which the virus is transmitted. Equally, changes in the acid stability of the virus may determine the organs in which the virus can readily replicate. For example, a virus's ability to spread into the low-pH environment of the digestive tract of the host may contribute to the lethality of the virus due to an increase in the number of organs where the virus can productively replicate. Equally, this may also determine the route of shedding of the virus, since this is a trait that has been shown to differ between H5N1 viruses (44). These are some of the factors that will be investigated in more detail in future work.

ACKNOWLEDGMENTS

We thank Elena Govorkova for generously providing the monoclonal antibodies. We thank Robert Lamb for the pCAGGS influenza virus Udorn HA plasmid and Karl-Klaus Conzelmann for the BSR-T7/5 cells. We thank Elena Govorkova for helpful discussions and Vani Shanker for editing the manuscript. We also thank Scott Krauss, Patrick Seiler and David Carey for technical support in the biosafety level 3 facility and the Hartwell Center shared resource at St. Jude Children's Research Hospital for sequencing data.

This project has been funded with federal funds from the National Institute Allergy and Infectious Diseases, National Institutes of Health, Department of Health and Human Services, under contract HHSN266200700005C and was supported by the American Lebanese Syrian Associated Charities.

REFERENCES

1. **Brown, J. D., D. E. Swayne, R. J. Cooper, R. E. Burns, and D. E. Stallknecht.** 2007. Persistence of H5 and H7 avian influenza viruses in water. Avian Dis. **51:**285–289.
2. **Buchholz, U. J., S. Finke, and K. K. Conzelmann.** 1999. Generation of bovine respiratory syncytial virus (BRSV) from cDNA: BRSV NS2 is not essential for virus replication in tissue culture, and the human RSV leader region acts as a functional BRSV genome promoter. J. Virol. **73:**251–259.
3. **Bullough, P. A., F. M. Hughson, J. J. Skehel, and D. C. Wiley.** 1994. Structure of influenza haemagglutinin at the pH of membrane fusion. Nature **371:** 37–43.
4. **Chang, D. K., and S. F. Cheng.** 2006. pH-dependence of intermediate steps of membrane fusion induced by the influenza fusion peptide. Biochem. J. **396:**557–563.
5. **Connor, R. J., Y. Kawaoka, R. G. Webster, and J. C. Paulson.** 1994. Receptor specificity in human, avian, and equine H2 and H3 influenza virus isolates. Virology **205:**17–23.
6. **Cross, K. J., S. A. Wharton, J. J. Skehel, D. C. Wiley, and D. A. Steinhauer.** 2001. Studies on influenza haemagglutinin fusion peptide mutants generated by reverse genetics. EMBO J. **20:**4432–4442.
7. **Daniels, R. S., J. C. Downie, A. J. Hay, M. Knossow, J. J. Skehel, M. L. Wang, and D. C. Wiley.** 1985. Fusion mutants of the influenza virus hemagglutinin glycoprotein. Cell **40:**431–439.
8. **de Jong, J. C., E. C. Claas, A. D. Osterhaus, R. G. Webster, and W. L. Lim.** 1997. A pandemic warning? Nature **389:**554.
9. **Doms, R. W., M. J. Gething, J. Henneberry, J. White, and A. Helenius.** 1986. Variant influenza virus hemagglutinin that induces fusion at elevated pH. J. Virol. **57:**603–613.
10. **Earp, L. J., S. E. Delos, H. E. Park, and J. M. White.** 2005. The many mechanisms of viral membrane fusion proteins. Curr. Top. Microbiol. Immunol. **285:**25–66.
11. **Gamblin, S. J., L. F. Haire, R. J. Russell, D. J. Stevens, B. Xiao, Y. Ha, N. Vasisht, D. A. Steinhauer, R. S. Daniels, A. Elliot, D. C. Wiley, and J. J. Skehel.** 2004. The structure and receptor binding properties of the 1918 influenza hemagglutinin. Science **303:**1838–1842.
12. **Garten, W., S. Hallenberger, D. Ortmann, W. Schafer, M. Vey, H. Angliker, E. Shaw, and H. D. Klenk.** 1994. Processing of viral glycoproteins by the subtilisin-like endoprotease furin and its inhibition by specific peptidylchloroalkylketones. Biochimie **76:**217–225.
13. **Gething, M. J., R. W. Doms, D. York, and J. White.** 1986. Studies on the mechanism of membrane fusion: site-specific mutagenesis of the hemagglutinin of influenza virus. J. Cell Biol. **102:**11–23.
14. **Gething, M. J., K. McCammon, and J. Sambrook.** 1986. Expression of wild-type and mutant forms of influenza hemagglutinin: the role of folding in intracellular transport. Cell **46:**939–950.
15. **Giannecchini, S., L. Campitelli, L. Calzoletti, M. A. De Marco, A. Azzi, and I. Donatelli.** 2006. Comparison of in vitro replication features of H7N3 influenza viruses from wild ducks and turkeys: potential implications for interspecies transmission. J. Gen. Virol. **87:**171–175.
16. **Ha, Y., D. J. Stevens, J. J. Skehel, and D. C. Wiley.** 2002. H5 avian and H9 swine influenza virus haemagglutinin structures: possible origin of influenza subtypes. EMBO J. **21:**865–875.
17. **Ha, Y., D. J. Stevens, J. J. Skehel, and D. C. Wiley.** 2003. X-ray structure of the hemagglutinin of a potential H3 avian progenitor of the 1968 Hong Kong pandemic influenza virus. Virology **309:**209–218.
18. **Ha, Y., D. J. Stevens, J. J. Skehel, and D. C. Wiley.** 2001. X-ray structures of H5 avian and H9 swine influenza virus hemagglutinins bound to avian and human receptor analogs. Proc. Natl. Acad. Sci. USA **98:**11181–11186.
19. **Hoffmann, E., G. Neumann, Y. Kawaoka, G. Hobom, and R. G. Webster.** 2000. A DNA transfection system for generation of influenza A virus from eight plasmids. Proc. Natl. Acad. Sci. USA **97:**6108–6113.
20. **Hoffmann, E., J. Stech, Y. Guan, R. G. Webster, and D. R. Perez.** 2001. Universal primer set for the full-length amplification of all influenza A viruses. Arch. Virol. **146:**2275–2289.
21. **Ilyushina, N. A., E. A. Govorkova, C. J. Russell, E. Hoffmann, and R. G. Webster.** 2007. Contribution of H7 haemagglutinin to amantadine resistance and infectivity of influenza virus. J. Gen. Virol. **88:**1266–1274.
22. **Kaverin, N. V., I. A. Rudneva, E. A. Govorkova, T. A. Timofeeva, A. A. Shilov, K. S. Kochergin-Nikitsky, P. S. Krylov, and R. G. Webster.** 2007. Epitope mapping of the hemagglutinin molecule of a highly pathogenic H5N1 influenza virus by using monoclonal antibodies. J. Virol. **81:**12911–12917.
23. **Kilpatrick, A. M., A. A. Chmura, D. W. Gibbons, R. C. Fleischer, P. P. Marra, and P. Daszak.** 2006. Predicting the global spread of H5N1 avian influenza. Proc. Natl. Acad. Sci. USA **103:**19368–19373.
24. **Klenk, H. D., R. Rott, M. Orlich, and J. Blodorn.** 1975. Activation of influenza A viruses by trypsin treatment. Virology **68:**426–439.
25. **Korte, T., K. Ludwig, F. P. Booy, R. Blumenthal, and A. Herrmann.** 1999. Conformational intermediates and fusion activity of influenza virus hemagglutinin. J. Virol. **73:**4567–4574.
26. **Lazarowitz, S. G., and P. W. Choppin.** 1975. Enhancement of the infectivity of influenza A and B viruses by proteolytic cleavage of the hemagglutinin polypeptide. Virology **68:**440–454.
27. **Lin, Y. P., S. A. Wharton, J. Martin, J. J. Skehel, D. C. Wiley, and D. A. Steinhauer.** 1997. Adaptation of egg-grown and transfectant influenza viruses for growth in mammalian cells: selection of hemagglutinin mutants with elevated pH of membrane fusion. Virology **233:**402–410.
28. **Luque, L. E., and C. J. Russell.** 2007. Spring-loaded heptad repeat residues regulate the expression and activation of paramyxovirus fusion protein. J. Virol. **81:**3130–3141.
29. **Markosyan, R. M., G. B. Melikyan, and F. S. Cohen.** 2001. Evolution of intermediates of influenza virus hemagglutinin-mediated fusion revealed by kinetic measurements of pore formation. Biophys. J. **80:**812–821.
30. **Puri, A., F. P. Booy, R. W. Doms, J. M. White, and R. Blumenthal.** 1990. Conformational changes and fusion activity of influenza virus hemagglutinin of the H2 and H3 subtypes: effects of acid pretreatment. J. Virol. **64:**3824–3832.
31. **Rogers, G. N., J. C. Paulson, R. S. Daniels, J. J. Skehel, I. A. Wilson, and D. C. Wiley.** 1983. Single amino acid substitutions in influenza haemagglutinin change receptor binding specificity. Nature **304:**76–78.
32. **Rott, R., and H. D. Klenk.** 1987. Significance of viral glycoproteins for infectivity and pathogenicity. Zentralbl. Bakteriol. Mikrobiol. Hyg. A **266:** 145–154.
33. **Russell, C. J., K. L. Kantor, T. S. Jardetzky, and R. A. Lamb.** 2003. A dual-functional paramyxovirus F protein regulatory switch segment: activation and membrane fusion. J. Cell Biol. **163:**363–374.
34. **Russell, C. J., and R. G. Webster.** 2005. The genesis of a pandemic influenza virus. Cell **123:**368–371.
35. **Russell, R. J., S. J. Gamblin, L. F. Haire, D. J. Stevens, B. Xiao, Y. Ha, and**

J. J. Skehel. 2004. H1 and H7 influenza haemagglutinin structures extend a structural classification of haemagglutinin subtypes. Virology **325:**287–296.
36. **Salomon, R., J. Franks, E. A. Govorkova, N. A. Ilyushina, H. L. Yen, D. J. Hulse-Post, J. Humberd, M. Trichet, J. E. Rehg, R. J. Webby, R. G. Webster, and E. Hoffmann.** 2006. The polymerase complex genes contribute to the high virulence of the human H5N1 influenza virus isolate A/Vietnam/1203/04. J. Exp. Med. **203:**689–697.
37. **Skehel, J. J., and D. C. Wiley.** 1998. Coiled coils in both intracellular vesicle and viral membrane fusion. Cell **95:**871–874.
38. **Skehel, J. J., and D. C. Wiley.** 2000. Receptor binding and membrane fusion in virus entry: the influenza hemagglutinin. Annu. Rev. Biochem. **69:**531–569.
39. **Steinhauer, D. A., J. Martin, Y. P. Lin, S. A. Wharton, M. B. Oldstone, J. J. Skehel, and D. C. Wiley.** 1996. Studies using double mutants of the conformational transitions in influenza hemagglutinin required for its membrane fusion activity. Proc. Natl. Acad. Sci. USA **93:**12873–12878.
40. **Steinhauer, D. A., S. A. Wharton, J. J. Skehel, and D. C. Wiley.** 1995. Studies of the membrane fusion activities of fusion peptide mutants of influenza virus hemagglutinin. J. Virol. **69:**6643–6651.
41. **Steinhauer, D. A., S. A. Wharton, J. J. Skehel, D. C. Wiley, and A. J. Hay.** 1991. Amantadine selection of a mutant influenza virus containing an acid-stable hemagglutinin glycoprotein: evidence for virus-specific regulation of the pH of glycoprotein transport vesicles. Proc. Natl. Acad. Sci. USA **88:**11525–11529.
42. **Stevens, J., O. Blixt, T. M. Tumpey, J. K. Taubenberger, J. C. Paulson, and I. A. Wilson.** 2006. Structure and receptor specificity of the hemagglutinin from an H5N1 influenza virus. Science **312:**404–410.
43. **Stevens, J., A. L. Corper, C. F. Basler, J. K. Taubenberger, P. Palese, and I. A. Wilson.** 2004. Structure of the uncleaved human H1 hemagglutinin from the extinct 1918 influenza virus. Science **303:**1866–1870.
44. **Sturm-Ramirez, K. M., D. J. Hulse-Post, E. A. Govorkova, J. Humberd, P. Seiler, P. Puthavathana, C. Buranathai, T. D. Nguyen, A. Chaisingh, H. T. Long, T. S. Naipospos, H. Chen, T. M. Ellis, Y. Guan, J. S. Peiris, and R. G. Webster.** 2005. Are ducks contributing to the endemicity of highly pathogenic H5N1 influenza virus in Asia? J. Virol. **79:**11269–11279.
45. **Takeda, M., G. P. Leser, C. J. Russell, and R. A. Lamb.** 2003. Influenza virus hemagglutinin concentrates in lipid raft microdomains for efficient viral fusion. Proc. Natl. Acad. Sci. USA **100:**14610–14617.
46. **Thoennes, S., Z. N. Li, B. J. Lee, W. A. Langley, J. J. Skehel, R. J. Russell, and D. A. Steinhauer.** 2008. Analysis of residues near the fusion peptide in the influenza hemagglutinin structure for roles in triggering membrane fusion. Virology **370:**403–414.
47. **Webster, R. G., and R. Rott.** 1987. Influenza virus A pathogenicity: the pivotal role of hemagglutinin. Cell **50:**665–666.
48. **Weis, W., J. H. Brown, S. Cusack, J. C. Paulson, J. J. Skehel, and D. C. Wiley.** 1988. Structure of the influenza virus haemagglutinin complexed with its receptor, sialic acid. Nature **333:**426–431.
49. **Weis, W. I., S. C. Cusack, J. H. Brown, R. S. Daniels, J. J. Skehel, and D. C. Wiley.** 1990. The structure of a membrane fusion mutant of the influenza virus haemagglutinin. EMBO J. **9:**17–24.
50. **Wharton, S. A., J. J. Skehel, and D. C. Wiley.** 1986. Studies of influenza haemagglutinin-mediated membrane fusion. Virology **149:**27–35.
51. **Wilson, I. A., J. J. Skehel, and D. C. Wiley.** 1981. Structure of the haemagglutinin membrane glycoprotein of influenza virus at 3 Å resolution. Nature **289:**366–373.
52. **Yamada, S., Y. Suzuki, T. Suzuki, M. Q. Le, C. A. Nidom, Y. Sakai-Tagawa, Y. Muramoto, M. Ito, M. Kiso, T. Horimoto, K. Shinya, T. Sawada, T. Usui, T. Murata, Y. Lin, A. Hay, L. F. Haire, D. J. Stevens, R. J. Russell, S. J. Gamblin, J. J. Skehel, and Y. Kawaoka.** 2006. Haemagglutinin mutations responsible for the binding of H5N1 influenza A viruses to human-type receptors. Nature **444:**378–382.
53. **Yoshimura, A., and S. Ohnishi.** 1984. Uncoating of influenza virus in endosomes. J. Virol. **51:**497–504.